1 **Phosphorus Recovery from Microbial Biofuel Residual Using Microwave Peroxide**

2 **Digestion and Anion Exchange**

3

4 McKay Gifford[a*], Jianyong Liu[b], Bruce E. Rittmann[c], Raveender Vannela[c], Paul

5 Westerhoff[a]

6

7 [*]Corresponding author:

8 [a]Arizona State University, School of Sustainable Engineering and The Built Environment,

9 Tempe, Box 5306, AZ 85287-5306; phone: 480-965-2885; fax: 480-965-0557; email:

10 mac.gifford@asu.edu

11

12 Affiliations

13 [a]Arizona State University, School of Sustainable Engineering and the Built Environment,

14 Tempe, AZ 85287-5306

15 [b]School of Environmental and Chemical Engineering, Shanghai University, 333 Nanchen

16 Road, Shanghai 200444, P. R. China

17 [c]Arizona State University, Swette Center for Environmental Biotechnology, Biodesign

18 Institute, Tempe, AZ 85287-5701

19

22

23 **Abstract**

24   Sustainable production of microalgae for biofuel requires efficient phosphorus (P)

25 utilization, which is a limited resource and vital for global food security. This research

26 tracks the fate of P through biofuel production and investigates P recovery from the

27 biomass using the cyanobacterium *Synechocystis* sp. PCC 6803. Our results show that

28 *Synechocystis* contained 1.4% P dry weight. After crude lipids were extracted (e.g., for

29 biofuel processing), 92% of the intracellular P remained in the residual biomass, indicating

30 phospholipids comprised only a small percentage of cellular P. We estimate a majority of

31 the P is primarily associated with nucleic acids. Advanced oxidation using hydrogen

32 peroxide and microwave heating released 92% of the cellular P into orthophosphate. We

33 then recovered the orthophosphate from the digestion matrix using two different types of

34 anion exchange resins. One resin impregnated with iron nanoparticles adsorbed 98% of

35 the influent P through 20 bed volumes, but only released 23% during regeneration. A

36 strong-base anion exchange resin adsorbed 87% of the influent P through 20 bed volumes

37 and released 50% of it upon regeneration. This recovered P subsequently supported

38 growth of *Synechocystis*. This proof-of-concept recovery process reduced P demand of

39 biofuel microalgae by 54%.

40

41 **Keywords**

42 Microbial Biofuel, Phosphorus Recovery, Oxidation, Anion Exchange, Iron Nanoparticles

43

1. Introduction

There is an urgent need to find energy replacements for fossil fuels, whose combustion releases known and suspected human carcinogens and greenhouse gases into the atmosphere. One promising alternative is biofuel, which provides renewable energy with net greenhouse gas emissions significantly lower than fossil fuel (Batan et al. 2010). Biofuel derived from microalgae offers several advantages over biofuel from terrestrial plants: it does not compete with food crops for arable land, it can be continuously harvested, and it provides a much higher areal yield (Rittmann 2008, Schenk et al. 2008).

Microalgae biofuel production requires several inputs, including water, sunlight, carbon dioxide, and nutrients – particularly nitrogen (N) and phosphorus (P). During lipid extraction from microalgae biomass for liquid fuels, most of the N and P are discarded, requiring new nutrients for subsequent growth. Should microalgae become a significant replacement for fossil fuel in the future, the requirements for biomass growth would create a huge nutrient demand, rivaling that of agriculture (Erisman et al. 2010). Thus, capturing and recycling nutrients represents a significant opportunity for making large-scale cultivation of microalgae more sustainable (Clarens et al. 2010).

Nutrient recycling is particularly essential for P. Unlike N, which can be fixed from the atmosphere through the Haber-Bosch method (Huo et al. 2012), P is mined from ore that has finite stocks. World reserves of accessible P are estimated as 65,000 million

Abbreviations: ATP, adenosine triphosphate, DI, deionized water; EBCT, empty bed contact time; FAME, fatty acid methyl esters; HAX, hybrid anion exchange; ortho-PO_4^{3-}, orthophosphate; P, phosphorus; PG, phosphatidylglycerol; SBAX, strong base anion exchange.

63   metric tons (USGS 2011), and these are non-renewable and not substitutable. Depletion

64   of economically affordable P may bring about international crises due to the essential role

65   of P fertilizer for global food production (Cordell et al. 2009). Farmers in developing

66   countries could be disproportionately harmed (Childers et al. 2011). Sustainable microbial

67   biofuel production demands efficient nutrient recycling to prevent biofuel from becoming

68   an enormous P demand competing with food production.

69   This research develops a proof-of-concept process for P-recovery from microalgae

70   after extraction of lipids. The research objective is to track P through biofuel production

71   and then recover P from residual biomass in a reusable form by using advanced oxidation

72   to release the P for efficient ion exchange capture. The reusable form provides

73   bioavailable P that supports microalgae growth.

74   We selected the cyanobacteria for this work because it is an excellent candidate for

75   future utilization in large-scale biomass cultivation, particularly when energy efficiency in

76   biosynthesis of fatty acids is crucial (Wijffels et al. 2013). Specifically we use

77   *Synechocystis* sp. PCC 6803, which is a prokaryotic autotroph, Gram negative and able to

78   withstand a wide range of environmental conditions. Lipids in the form of diacylglycerols

79   are available in an extensive network of thylakoid membranes (van de Meene et al. 2006,

80   Vermaas 2001).   It may be genetically manipulated for specific traits favorable for biofuel

81   production such as high lipid content (Vermaas 1996) because the entire genome has been

82   sequenced (Kaneko et al. 1996).

83

84   *1.1. P Recovery*

85   To recover P from microbial biomass we first release organic-bound P as inorganic

86   orthophosphate (ortho-PO_4^{3-}). This is necessary to improve the efficiency of the

87   subsequent capture since ortho-PO_4^{3-} is more reactive. It also mitigates heterotrophic

88   contamination of the biomass culture, which can occur after long run periods or with

89   accumulation of inactive cells (Mata et al. 2010). Subsequently, we selectively capture the

90   ortho-PO_4^{3-} from the liquid in a usable form. This is necessary to isolate and purify the

91   ortho-PO_4^{3-}, allowing accurate and controlled dosing into the aqueous growth media during

92   reuse. It also concentrates the ortho-PO_4^{3-} solution to minimize handling or hauling. This

93   subsection gives the impetus for the technologies we selected to accomplish those goals.

94   Many P-recovery methods are available (de-Bashan and Bashan 2004, Morse et al.

95   1998, Rittmann et al. 2011).   We selected an advanced oxidation process using hydrogen

96   peroxide and microwave heating to release organic P from the residual biomass. Advanced

97   oxidation creates hydroxyl free radicals that are highly effective for attacking organic

98   matter to release ortho-PO_4^{3-} (Liao et al. 2005). This transformation may involve oxidation

99   and hydrolysis reactions. While it may be possible to find technologies that are less

100   energy-intensive, such as enzymatic hydrolysis or microbial fuel cells (Rittmann et al.

101   2011), or that do not dilute the biomass with additional liquid such as supercritical carbon

102   dioxide (Blocher et al. 2012, Soh and Zimmerman 2011), advanced oxidation demonstrates

103   the principle for releasing PO_4^{3-}.

104   We capture ortho-PO_4^{3-} using ion exchange since it recovers a liquid concentrate

105   that is preferable for nutrient reuse during aquatic microalgae production. Other common

106   recovery techniques such as aluminum adsorption or struvite precipitation (de-Bashan and

107   Bashan 2004) produce complex or low solubility solids which may be better suited for

108 agricultural application. We evaluated two anion-exchange resins having distinctly

109 different properties. The first was a hybrid anion exchange resin (HAX) impregnated with

110 iron (hydr)oxide nanoparticles (Layne RT, Layne Christensen). It is reported to have a

111 high sorption capacity and selectivity for ortho-PO_4^{3-} (Sengupta 2013) and the ability to

112 release a high concentration ortho-PO_4^{3-} solution upon regeneration (Blaney et al. 2007,

113 Midorikawa et al. 2008). The second was a type-1 strong-base anion exchange resin

114 (SBAX) with quaternary amine functional groups in chloride ion form (21K-XLT,

115 Dowex). It has a general anion-exchange capacity of 1.4 equivalents/L. It has previously

116 been used for uranium (Stucker et al. 2011) and chromium (Rees-Nowak et al. 2005)

117 removal, but has yet to be tested for phosphate recovery.

118 While the individual P recovery technologies employed in this study are not novel

119 by themselves, their usage together such that the P completes an entire use and reuse cycle

120 is. It is also the first study we know of to apply these technologies in the context of

121 microbial biofuel production. Thus this study serves as a proof-of-concept that proposes

122 an approach and can inform future optimization.

123

124 *1.2. Microbial P*

125 To focus the recovery efforts properly, this subsection estimates where P in

126 *Synechocystis* is located based on literature review. Others have done this for several

127 marine microalgae (Geider and La Roche 2002, Sterner and Elser 2002) but not

128 specifically for *Synechocystis*. Biochemical fractions in cells can vary based on growth

129 conditions (Sheng et al. 2011a) but this provides clues for understanding the fate of P after

130 lipid processing. Figure 1 summarizes the expected location of P in a *Synechocystis* cell.

131   P may be located within adenosine triphosphate (ATP), lipids, and nucleic acid. The

132   following three paragraphs individually analyze them.

133   ATP contains over 18% P by weight ($C_{10}H_{16}N_5O_{13}P_3$), but comprises less than 30

134   µg per g of cell mass. P associated with ATP is therefore 5 µg per g of the cell mass,

135   which is a negligible contributor of the total cell P. The diphosphate form ADP and

136   monophosphate form AMP are smaller fractions of the cell mass with less incorporated P

137   and are also negligible contributors of cellular P storage.

138   The P content associated with lipid is a function of the fraction of lipid that is

139   phospholipid and the fraction of phospholipid that is P. The predominant phospholipid

140   head within cyanobacteria is phosphatidylglycerol (PG), which is the only phospholipid

141   associated with thylakoid membranes in *Synechocystis* sp. PCC 6803 (Hajime and Murata

142   2007). PG has an elemental composition of $C_8H_{12}O_{10}P$. The most prevalent fatty acid

143   chain in *Synechocystis* is C16:0, or palmitic acid (Sheng et al. 2011b), which has an

144   elemental composition of $C_{16}H_{32}O_2$. Assuming that all phospholipids within *Synechocystis*

145   are the diacylglycerol PG with two palmitic acid molecules, the overall elemental formula

146   for a phospholipid molecule is $C_{40}H_{76}O_{14}P$. That means phospholipid is approximately

147   3.8% P by weight. PG-based lipids comprise approximately 14% of all lipids in

148   *Synechocystis* (Sakurai et al. 2006), and lipids represent approximately 10% of the

149   biological makeup of the overall cell (Shastri and Morgan 2005). Combining these

150   estimates gives the theoretical amount of P associated with lipid in *Synechocystis* sp. PCC

151   6803 as 0.05% of the total cell weight, or 2% of the total cell P. A genetically altered high

152   lipid strain containing 50% crude lipids could then have as high as 0.3% of the total cell

153   weight be P associated with lipid. For this reason, we do not expect much P in the lipids.

154   We estimate the P content associated with DNA and RNA by comparing its

155   biological composition with its elemental composition. *Synechocystis* sp. PCC 6803 is

156   approximately 3% DNA and 17% RNA by weight (Shastri and Morgan 2005). DNA and

157   RNA are 10% P by weight (Sterner and Elser 2002). Therefore, P associated with DNA

158   comprises 0.3% of the total cell weight, and P associated with RNA is 1.7% of the total

159   cell weight. This is respectively 15% and 83% of the total cellular P. We consequently

160   expect that most of the cellular P will be in nucleic acid. This was also observed in other

161   studies on lake bacteria where P associated with RNA comprised a majority of the total

162   cell P (Elser et al. 2003, Geider and La Roche 2002).

163

164

165   **2. Materials and Methods**

166   *2.1. Strain, Growth Conditions, and Biomass Production*

167   We grew *Synechocystis* sp. PCC 6803 in BG-11 growth media (Rippka et al. 1979)

168   modified to have five times the normal amount of phosphate (added as K_2HPO_4) (Kim et

169   al. 2010) in a bench-top photobioreactor in semi-continuous growth mode. We separated

170   biomass from the growth medium by means of centrifugation at 1,500 g for 20 min in 50-

171   mL plastic tubes. We resuspended the cell pellet in 1 mM sodium bicarbonate (Sigma-

172   Aldrich) to rinse away residual medium. We repeated centrifuging and rinsing two times

173   before freeze-drying the final pellet (Labconco Freezone 6) for 2 days at 0.013 mbar and -

174   50ºC in order to obtain an accurate starting dry weight (Sheng et al. 2011b). We collected

175   enough biomass to perform all lipid extraction and P recovery experiments at least in

176   duplicate.

177

178   *2.2. Lipid Extraction and Transesterification*

179   We extracted lipids from the freeze-dried biomass using the Folch Method (Folch

180   et al. 1957) using a 2:1 (V:V) mixture of chloroform (Mallinckrodt) and methanol (Fisher

181   Scientific), since it has a high extraction efficiency for *Synechocystis* lipids (Sheng et al.

182   2011b). We ground a 300-mg (all weights given as dry weight) sample with agate mortar

183   and pestle, suspended it in 60 mL of Folch solvent, and placed it on a shaker table at 175

184   rpm for 2 days. We filtered the suspension with a glass fiber filter (Whatman GF/B) and

185   then a 0.2-µm polytetrafluoroethylene filter (Whatman). The biomass retained on both

186   filters was the primary residual, and the filtrate contained the extracted crude lipid. For

187   samples undergoing transesterification, we evaporated the solvent from the crude lipid

188   under N_2 gas to avoid oxidation of lipids. For samples where no further lipid processing

189   was necessary, we evaporated the solvent by heating on hot plate.

190   We transesterified the crude lipid (Sheng et al. 2011b) by adding 1 mL of

191   methanolic hydrochloric acid (Supelco) and heating the mixture in an 85ºC water bath for

192   2 h. After cooling the mixture to room temperature, we added 0.5 mL of deionized (DI)

193   water and 1 mL of hexane, shook the mixture by hand for 30 s, and allowed the phases to

194   separate. We repeated all transesterification steps two additional times, and then pooled all

195   the hexane. The extracted hexane contained the fatty acid methyl esters (FAME), and the

196   remaining water contained the secondary residual.

197   For experiments tracking the fate of P, we analyzed total P for each biomass,

198   primary residual, crude lipid, secondary residual, and transesterified FAME (at least

199   duplicate samples).

200

2.3. Advanced Oxidation

We scraped primary residual from the dried filters and added it to 60 mL (giving

3.6 gVSS/L) of 30% ultrapure H_2O_2 solution (JT Baker Ultrex II) diluted 1:10. We let this

mixture stand for 1 hr of pre-digestion under fume-hood ventilation. We digested the

mixtures in a microwave (CEM MARS XPress) at 400 W by ramping the temperature up

to 170ºC over 10 min and then holding at 170ºC for 10 min per method SW846-3015

(USEPA 2008). Others have observed the highest fraction of P release by this peroxide

dose and microwave heating temperature (Liao et al. 2005, Wong et al. 2006), and future

work may explore varying other conditions to optimize P release. We employed high-

pressure microwave vessels to avoid breakage that the high rate of gas evolution could

cause. We analyzed duplicate samples before and after oxidation for total P and ortho-

PO_4^{3-}.

2.4. Phosphate Separation

We did preliminary investigation of the P separation capacity of each of the two

anion exchange resins by placing 3.5 g of fresh resin in a 1.5-cm inner diameter glass

column, giving a bed depth of 3.0 cm. We supported the resin with glass beads to ensure

even flow distribution. We flushed 100 mL of DI water through the column and allowed

air bubbles to escape. Then, we pumped a solution of monobasic sodium phosphate

(Mallinkrodt ACS grade) in DI water (concentration 80 mgP/L) through the column at 3.2

mL/min to give an empty bed contact time (EBCT) of approximately 2 min (loading rate of

4.4 mgP/s/g resin). We periodically took effluent samples for P analysis, and continued

223 the experiment until the effluent P concentration stabilized near the influent P

224 concentration. We then desorbed the P using a strong regeneration solution at a pump rate

225 of 0.5 mL/min (EBCT of approximately 10 min) until the effluent P concentration

226 stabilized at nearly zero. The strong regeneration solution used for the HAX resin was 0.1

227 N potassium hydroxide (EMD), and for the SBAX resin was 0.1 N sodium chloride (Sigma

228 Aldrich). We later varied influent P concentration, EBCT, P loading rate, influent pH, and

229 elute contact time in order to optimize column operation.

230 We then tested each resin with biomass after advanced oxidation by pumping the

231 60 mL of digested sample through 2.0 g of fresh resin having a bed depth of 1.7 cm. The

232 flow rate was 1.4 mL/min, giving an EBCT of approximately 2 min. We collected the

233 effluent and pumped it through the column two more times to ensure complete capture of

234 phosphate onto the resin. We then recovered retained ortho-PO_4^{3-} by removing the resin

235 from the column and placing it in 33 mL (11 bed volumes) of strong regeneration solution,

236 which was heated on a 95ºC hot plate, shaken for 24 h, and then decanted. Elution and

237 decanting were repeated two times, and the elution solutions were pooled so that the serial

238 batch elution mimicked a continually stirred tank mixer (CSTM) in series (n = 3). We

239 analyzed the total volume of 100 mL (33 bed volumes) for pH, total P, and ortho-PO_4^{3-}.

240 We obtained the total mass of P sorbed to each resin by summing the difference

241 between the influent concentration and the effluent concentration for each sample

242 multiplied by the volume treated in the time segment (area above the curve times flow

243 rate).

244

245 *2.5. Phosphorus Reuse*

246   As a confirmatory experiment, recovered P solution was used to culture wild-type

247   *Synechocystis* sp. PCC 6803 cells. We diluted the recovered P solution to P concentration

248   prescribed by standard BG-11, spiked the other nutrients to standard levels, then added

249   additional bicarbonate to compensate for low aeration in small samples. We inoculated

250   plastic tubes containing 20 mL of the growth media with fresh *Synechocystis* cells in

251   duplicate. We placed these on a shake table under constant light conditions for one week,

252   and regularly monitored optical density by absorbance at 730 nm.

253

254   *2.6. Phosphorus Analysis*

255   We determined ortho-PO_4^{3-} colorimetrically with a spectrophotometer (HACH

256   DR5000) using the PhosVer 3 Method (HACH), which is equivalent to *Standard Methods*

257   4500-P.E (Miner 2006). It directs to add reagent powder to 5 mL of sample and give 2

258   min of reaction time, then measure results at 880 nm.

259   We assayed total P by persulfate digestion (*Standard Method* 4500-P.B.5) (Miner

260   2006) followed by inductively coupled plasma optical emission spectrometry (ICP-OES).

261   To do this we suspended samples in 50 mL DI water plus 1 mL of concentrated sulfuric

262   acid (JT Baker ultrapure). We then added 0.4 mg of ammonium persulfate (Malinckrodt)

263   to each sample. We autoclaved the sample for 30 min at a pressure of 1.05 kg/cm^2 and a

264   temperature of 122ºC. We measured total P by ICP-OES (Thermo iCAP6300) at a

265   wavelength of 213.6 nm.

266

267   **3. Results & Discussion**

268   *3.1. Fate of P through lipid extraction*

269   Freeze dried *Synechocystis* sp. PCC 6803 biomass contained 1.39%±0.28% total P

270   by dry mass. (All weights given by dry weight. ± indicates half standard deviation.) This

271   is consistent with previous findings that P is 1.5% of dry cell mass (Kim et al. 2010). In

272   lipid-extracted biomass samples, primary residual contained 1.50%±0.36% total P by dry

273   mass. Figure 2 summarizes the fate of P through lipid extraction normalized to 100 mg of

274   total P in the starting biomass. The primary residual contained 92±4.3 mg total P. Crude

275   lipid contained 7.3±4.2 mg total P. For transesterified samples, total P in the FAME was

276   0.5±0.1 mg total P. Total P in the secondary residual was 9.5±5.3 mg. Thus, nearly all of

277   the starting organic P was in the primary residual after lipid extraction. Of the small

278   amount in the crude lipids, nearly all of it was in the secondary residual. Essentially no P

279   (<1% of the starting P) was in the transesterified FAME.

280   These findings support our expectation that nucleic acid is the primary storage of

281   total cell P, with only small amounts stored in phospholipids. P associated with

282   phospholipid partitions to the crude lipid during extraction, while P associated with nucleic

283   acid remains in the primary residual. This explains the large fraction of P found

284   experimentally in the primary residual. The observed increase in P content from dry cells

285   to primary residual (1.39±0.28% to 1.50±0.36%) was not statistically significant, but any

286   increase would demonstrate the disproportional storage of P in non-lipid structures. The

287   92±4% of P found experimentally in the residual correlates with the expected 98% P

288   associated with nucleic acid. We attribute the small amount of P found in the fatty acids to

289   impurities from incomplete partitioning and analytical margin of error.

290

291   *3.2. Oxidation of Organic P to Release Ortho-PO$_4^{3-}$*

292   Since only small amounts of the starting P were in the crude lipid and subsequent

293   lipid processing, the primary residual became the focus for P recovery. Prior to treatment

294   with H_2O_2 and microwave heating, this primary residual contained 82±1 mg total P with

295   0.2 mg of it as ortho-PO_4^{3-}. After H_2O_2 and microwave treatment, samples contained

296   90±12 mg total P, including 75±6 mg as ortho-PO_4^{3-}. Therefore, H_2O_2 oxidation recovered

297   106±17% of the total P (analytical error accounts for recovery over 100%) and released

298   most of it as ortho-PO_4^{3-}, which was the objective.

299

300   *3.3. Recovery of Ortho-PO_4^{3-} by Resins from DI Water*

301   Figure 3A shows the ability of the two resins to absorb P in DI water. Both resins

302   were able to capture nearly all of the influent P up to 30 bed volumes. At this point, the

303   capacity of the resins was 5.0 mgP/g resin and 4.7 mgP/g resin for the HAX and SBAX

304   resins, respectively. The HAX resin then began a sharp breakthrough and reached

305   complete saturation near 80 bed volumes. The SBAX resin began a gradual breakthrough,

306   reaching 50% saturation around 200 bed volumes and 80% saturation around 500 bed

307   volumes. At the end of the experiments, the HAX resin sorbed a total mass of 38 mg of P,

308   giving a sorption capacity of 11 mgP/g resin, and the SBAX resin sorbed a total mass of

309   140 mg of P, giving a sorption capacity of 40 mgP/g resin.

310   Both resins released all of the P that would be eluted within the first 20 bed

311   volumes of regeneration. They did not release any additional P with 10 additional bed

312   volumes of regeneration (Figure 3B). The fastest rate of P elution for the SBAX resin

313   occurred around 5 bed volumes, and around 8 bed volumes for the HAX resin. A total of

314   19 mg of P was eluted from the HAX resin, or 51% of the total sorbed P was recovered. A

315 total of 167 mg of P was eluted from the SBAX resin, or 119% of the total sorbed was

316 recovered (the lack of mass-balance closure was due to analytical error from high dilution

317 required for analysis of concentrated elute). The pH of the HAX elute containing the

318 recovered P was 12, and of the SBAX elute it was 6.

319   The HAX resin had higher selectivity for P as demonstrated by the lower amount of

320 P in the column effluent, the sharp breakthrough curve showing a short saturation zone,

321 and the higher sorption capacity. We therefore expect it to have a higher rate of P capture

322 in solutions with competing constituents like the oxidized biomass. However, 0.1 N KOH

323 did not efficiently recover the sorbed P. While the iron nanoparticles lead to higher

324 sorption capacity than SBAX, they apparently made it more difficult to desorb the P. Poor

325 recovery might indicate that at least part of the sorbed P was irreversibly adsorbed by the

326 impregnated iron (hydr)oxide nanoparticles instead of sorbed entirely by anion exchange.

327 Our result differs from previous studies that showed that 80-90% of the P could be released

328 by elution from the HAX resin (Martin et al. 2009, Sengupta 2013) using 0.5-1.0 N NaOH

329 plus 0.4 N NaCl. Differences with these previous studies include different influent

330 matrices, not using combined NaCl and NaOH elutes or in as strong doses, and lower resin

331 contact time. We avoided stronger eluent doses so the recaptured P would not be in such a

332 high saline or high pH matrix that it would be unsuitable for subsequent microbial growth.

333 Since elution of the SBAX resin with 0.1 N NaCl showed the best recovery, we focused

334 our subsequent ion-exchange work on it.

335   In order to improve performance with the SBAX resin, we varied column operation

336 parameters to improve the P capture and release. For P capture, a steep breakthrough

337 curve is desired so that all of the P is captured until the inception of breakthrough, at which

338 time the column is stopped and regenerated. The SBAX breakthrough curve could be

339 made steeper by lowering the hydraulic loading rate. Figure 4 shows results for a SBAX

340 column receiving 100 mgP/L influent in DI water with an EBCT of 20 min (instead of 2

341 min) and a lower hydraulic loading rate of 3 BV/hr (instead of 30 BV/hr). Consequently,

342 the resin captured all ortho-PO_4^{3-} for 200 BV before exhibiting a steep and desirable

343 breakthrough curve. This gave a sorption capacity of 35.6 mgP/g resin. For P

344 regeneration, slower elution (2 BV/hr) gave 99% recovery of the loaded P within 4 BVs.

345 This allowed us to achieve an 80-fold increase in P concentration in the regenerant.

346 Additional tests (data not shown) indicated greater ortho-PO_4^{3-} exchange capacity at pH 5

347 instead of 8. This effort aimed to show that each step in this proof-of-concept P-recovery

348 sequence could be optimized to obtain desired performance outcomes.

349

350 *3.4. Recovery of Ortho-PO_4^{3-} by Resins from Oxidized Biomass*

351   We pumped oxidized primary residual through the ion exchange columns with

352 enough resin so the influent did not exceed 20 bed volumes to ensure complete capture of

353 the P. The HAX column effluent contained 1.7±0.3 mg of P out of the 72±0.9 mgP

354 influent, indicating 98% P capture on the resin. After elution, 16.7±0.0 mg P was in the

355 100 mL elute. Of this, 14.9±0.1 mg was ortho-PO_4^{3-}. The pH of the pooled elute was

356 12.4±0.5. Overall, the HAX resin recovered 23%±0.2% of the influent P to the

357 regeneration solution.

358   The SBAX column effluent contained 20.9±7.6 mg of P out of 108±7.6 mgP

359 influent, indicating 81% of the P sorbed to the resin. After elution, 54.4±8.9 mg of P was

360 in the 100 mL elute. Of this, 53.0±8.2 mg was ortho-PO_4^{3-}. The pH of the pooled elute

361   was 6.6±0.1. Overall, the SBAX resin recovered 50%±5% of the influent P to the

362   regeneration solution.

363   Both resins were only able to recover about half as much P when loaded from

364   oxidized biomass as opposed to when loaded from DI water: HAX went from 51% to

365   23%, and SBAX went from 119% to 50%. Previous studies have also observed lower

366   recovery from complex solutions like sludge liquor than from synthetic solutions (Bottini

367   and Rizzo 2012). In addition to ortho-PO_4^{3-}, the solutions from the oxidized biomass also

368   contained residual organic matter (after oxidation 15 mg P out of 90 mg P was still

369   organic-bound) and other anions (bicarbonate, carbonate, sulfate, and nitrate) that were

370   probably also exchanged by the resins. Additionally, the influent pH for DI tests was 5,

371   but for influent oxidized biomass it was over 6. Having the pH approach the second

372   deprotonation for ortho-PO_4^{3-} ($pK_{a,2} = 7.2$) during loading shifted a small fraction of its

373   speciation away from the single charge $H_2PO_4^-$ to the double charged HPO_4^{-2}. This may

374   have reduced ortho-PO_4^{3-} adsorption capacity because each HPO_4^{-2} takes up two anion-

375   exchange sites. This effect would be even stronger during regeneration due to the higher

376   pH (12 for the HAX) of the elute when almost all of the ortho-PO_4^{3-} would be present as

377   HPO_4^{-2}. In the case of the HAX resin, this competition for anion exchange sites may have

378   forced more ortho-PO_4^{3-} to be sorbed to the iron (hydr)oxide nanoparticles which could

379   form inner sphere complexes with stronger bonding and less elution.

380

381   *3.5. P Recovery and Reuse*

382   Figure 5 summarizes results for each process step in the overall recovery process

383   using the SBAX resin. The lipid extraction, cellular oxidation, and nutrient isolation steps

384   were, respectively, able to recover 93%, 106%, and 50% (using SBAX) of the starting P.

385   The overall process recovered 54% of the starting intracellular P into a pure and

386   concentrated nutrient solution. This yield is similar to other systems designed for complete

387   P recovery (Blocher et al. 2012) and shows that nutrient reuse in the context of microalgae

388   biofuel production is viable.

389   The recovered solution had an ortho-PO_4^{3-} concentration of 10.6 mgP/L, compared

390   to 5.4 mgP/L required in standard BG-11. We also measured 0.95 mg NO_3^--N/L and 1.5

391   mg SO_4^{2-}-S/L, compared to 247 and 9.8 mg/L required for BG-11, respectively,

392   demonstrating the selectivity of the resin for P.

393   The P solution recovered from the SBAX supported cyanobacteria growth. The

394   optical density increased from 0.12 initially to 0.55 after one day and to 1.11 after one

395   week. This correlates to specific growth rates of 1.4 day^{-1} over one day and 0.7 day^{-1} over

396   one week. For comparison, the optical density of the same cell culture grown in a BG-11

397   solution without any P went from 0.12 initially to 0.16 after one day and 0.10 after one

398   week, corresponding to specific growth rates of 0.26 day^{-1} after one day and -0.06 day^{-1}

399   after one week. The nearly ten-fold increase in cell density over one week in the solution

400   containing recovered P confirms that the recovered P was available for cyanobacteria

401   uptake. It also demonstrates that we did not co-recover any substances that would inhibit

402   reuse, such as harmful heavy metals or residual oxidant. These rates are comparable to

403   growth rates previously observed for *Synechocystis* using BG-11 (Kim et al. 2010) albeit in

404   a different reactor configuration.

405   We recommend future work improving P release methods that can co-recover other

406   valuable products produced by cyanobacteria, like other nutrients, proteins, or ethanol

407 (Wijffels et al. 2013). We further recommend improving P capture efficiency, reducing the

408 overall cost, energy, and chemical footprint of the process, and demonstrating recovery on

409 full-scale. Other future work could compare the effectiveness of growing microalgae on

410 recovered P compared to other sources of P with complete controls.

411

412 **4. Conclusions**

413 Efficient P recycling in microbial biofuel production will be essential to preventing

414 competition between food and energy systems. This work demonstrates:

415 • After lipid processing, over 90% of the P remained in the residuals. Most cellular P

416 is in nucleic acids, with very little in phospholipids.

417 • Advanced oxidation transformed over 80% of that organic P into useful and

418 recoverable ortho-PO_4^{3-}.

419 • While HAX resin showed higher affinity for ortho-PO_4^{3-}, the SBAX resin released

420 the ortho-PO_4^{3-} more completely.

421 • Both resins recovered less P from oxidized biomass than from P spiked DI water,

422 likely due to interference with residual organics or competing oxyanions.

423

431

432 **References**

433 Batan, L., Quinn, J., Willson, B. and Bradley, T. (2010) Net Energy and Greenhouse Gas

434   Emission Evaluation of Biodiesel Derived from Microalgae. Environmental

435   Science and Technology 44(20), 7975-7980.

436 Blaney, L.M., Cinar, S. and Sengupta, A.K. (2007) Hybrid Anion Exchanger for Trace

437   Phosphate Removal from Water and Wastewater. Water Research 41(7), 1603-

438   1613.

439 Blocher, C., Niewersch, C. and Melin, T. (2012) Phosphorus Recovery from Sewage

440   Sludge with a Hybrid Process of Low Pressure Wet Oxidation and Nanofiltration.

441   Water Research 46(6), 2009-2019.

442 Bottini, A. and Rizzo, L. (2012) Phosphorus Recovery from Urban Wastewater Treatment

443   Plant Sludge Liquor by Ion Exchange. Separation Science & Technology 47(4),

444   613-620.

445 Childers, D.L., Corman, J., Edwards, M. and Elser, J.J. (2011) Sustainability Challenges of

446   Phosphorus and Food: Solutions from Closing the Human Phosphorus Cycle.

447   Bioscience 61(2), 117-124.

448 Clarens, A.F., Resurreccion, E.P., White, M.A. and Colosi, L.M. (2010) Environmental

449   Life Cycle Comparison of Algae to Other Bioenergy Feedstocks. Environmental

450   Science & Technology 44(5), 1813-1819.

451 Cordell, D., Drangert, J. and White, S. (2009) The Story of Phosphorus: Global Food

452   Security and Food for Thought. Global Environmental Change 19(2), 292-305.

453 de-Bashan, L.E. and Bashan, Y. (2004) Recent advances in removing phosphorus from

454   wastewater and its future use as fertilizer (1997-2003). Water Research 38(19),

455   4222-4246.

456 Elser, J.J., Acharya, K., Kyle, M., Cotner, J., Makino, W., Markow, T., Watts, T., Hobbie,

457   S., Fagan, W., Schade, J., Hood, J. and Sterner, R.W. (2003) Growth Rate

458   Stoichiometry Couplings in Diverse Biota. Ecology Letters 6(10), 936-943.

459 Erisman, J.W., van Grinsven, H., Leip, A., Mosier, A. and Bleeker, A. (2010) Nitrogen and

460   biofuels; an overview of the current state of knowledge. Nutrient Cycling in

461   Agroecosystems 86(2), 211-223.

462 Folch, J., Lees, M. and Stanley, G.H.S. (1957) A Simple Method for the Isolation and

463   Purification of Total Lipids from Animal Tissues. Journal of Biological Chemistry

464   226(1), 497-509.

465 Geider, R. and La Roche, J. (2002) Redfield revisited: Variability of C:N:P in marine

466   microalgae and its biochemical basis. European Journal of Phycology 37(1), 1-17.

467 Hajime, W. and Murata, N. (2007) The Essential Role of Phosphatidylglycerol in

468   Photosynthesis. Photosynthesis Research 92(2), 205-215.

469 Huo, Y.-X., Wernick, D.G. and Liao, J.C. (2012) Toward nitrogen neutral biofuel

470   production. Current Opinion in Biotechnology 23(3), 406-413.

471 Kaneko, T., Sato, S., Kotani, H., Tanaka, A., Asamizu, E., Nakamura, Y., Miyajima, N.,

472   Hirosawa, M., Sugiura, M., Sasamoto, S., Kimura, T., Hosouchi, T., Matsuno, A.,

473   Muraki, A., Nakazaki, N., Naruo, K., Okumura, S., Shimpo, S., Takeuchi, C.,

474   Wada, T., Watanabe, A., Yamada, M., Yasuda, M. and Tabata, S. (1996) Sequence

475   Analysis of the Genome of the Unicellular Cyanobacterium Synechocystis sp.

476   Strain PCC6803. II. Sequence Determination of the Entire Genome and

477   Assignment of Potential Protein-coding Regions. DNA Research 3(3), 109-136.

478 Kim, W.K., Vannela, R., Zhou, C., Harto, C. and Rittmann, B.E. (2010) Photoautotrophic

479   Nutrient Utilization and Limitation During Semi-Continuous Growth of

480   Synechocystis sp. PCC6803. Biotechnology and Bioengineering 106(4), 553-563.

481 Liao, P.H., Wong, W.T. and Lo, K.V. (2005) Advanced Oxidation Process Using

482   Hydrogen Peroxide/Microwave System for Solubilization of Phosphate. Journal of

483   Environmental Science and Health 40(9), 1753-1761.

484 Martin, B.D., Parsons, S.A. and Jefferson, B. (2009) Removal and Recovery of Phosphate

485   from Municipal Wastewater Using a Polymeric Anion Exchanger Bound with

486   Hydrated Ferric Oxide Nanoparticles. Water Science and Technology 60(10),

487   2637-2645.

488 Mata, T.M., Martins, A.A. and Caetano, N.S. (2010) Microalgae for Biodiesel Production

489   and Other Applications: A Review. Renewable & Sustainable Energy Reviews

490   14(1), 217-232.

491 Midorikawa, I., Aoki, H., Omori, A., Shimizu, T., Kawaguchi, Y., Kassai, K. and

492   Murakami, T. (2008) Recovery of High Purity Phosphorus from Municipal

493   Wastewater Secondary Effluent by a High Speed Adsorbent. Water Science and

494   Technology 58(8), 1601-1607.

495 Miner, G. (2006) Standard Methods for the Examination of Water and Wastewater, 21st

496   Edition, American Water Works Association.

497 Morse, G.K., Brett, S.W., Guy, J.A. and Lester, J.N. (1998) Review: Phosphorus Removal

498   and Recovery Technologies. The Science of the Total Environment 212(1), 69-81.

499 Rees-Nowak, D., Marston, C. and Gisch, D. (2005) Controlling Chromium. Water &

500   Wastewater International 20(5), 21.

501 Rippka, R., Deruelles, J., Waterbury, J.B., Herdman, M. and Stanier, R.Y. (1979) Generic

502   Assignments, Strain Histories And Properties Of Pure Cultures Of Cyanobacteria.

503   Journal of General Microbiology 111(Mar), 1-61.

504 Rittmann, B.E. (2008) Opportunities for renewable bioenergy using microorganisms.

505   Biotechnology and Bioengineering 100(2), 203-212.

506 Rittmann, B.E., Mayer, B., Westerhoff, P. and Edwards, M. (2011) Capturing the lost

507   phosphorus. Chemosphere 84(6), 846-853.

508 Sakurai, I., Shen, J., Leng, J., Ohashi, S., Kobayashi, M. and Wada, H. (2006) Lipids in

509   Oxygen Evolving Photsystems II Complexes of Cyanobacteria and Higher Plants.

510   Journal of Biochemistry 140(2), 201-209.

511 Schenk, P.M., Thomas-Hall, S.R., Stevens, E., Marx, U.C., Mussgnug, J.H., Posten, C.,

512   Kruse, O. and Hankamer, B. (2008) Second Generation Biofuels: High Efficiency

513   Microalgae for Biodiesel Production. Bioenergy Research 1(1), 20-43.

514 Sengupta, S. (2013) Novel Solutions to Water Pollution. Ahuja, S. and Hristovski, K.

515   (eds), pp. 167-187, American Chemical Society, Washington DC.

516 Shastri, A.A. and Morgan, J.A. (2005) Flux Balance Analysis of Photoautotrophic

517   Metabolism. Biotechnology 21(6), 1617-1626.

518 Sheng, J., Kim, H.W., Badalamenti, J.P., Zhou, C., Sridharakrishnan, S., Krajmalnik-

519   Brown, R., Rittmann, B.E. and Vannela, R. (2011a) Effects of Temperature Shifts

520   on Growth Rate and Lipid Characteristics of Synechocystis sp. PCC6803 in a

521   Bench-Top Photobioreactor. Bioresource Technology 102(24), 11218-11225.

522   Sheng, J., Vannela, R. and Rittmann, B.E. (2011b) Evaluation of Methods to Extract and

523   Quantify Lipids from Synechocystis PCC6803. Bioresource Technology 102(2),

524   1697-1703.

525   Soh, L. and Zimmerman, J. (2011) Biodiesel Production: The Potential of Algal Lipids

526   Extracted with Supercritical Carbon Dioxide. Green Chemistry 13(6), 1422-1429.

527   Sterner, R.W. and Elser, J.J. (2002) Ecological Stoichiometry: The Biology of Elements

528   from Molecules to the Biosphere, Princeton University Press, Princeton, New

529   Jersey.

530   Stucker, V., Ranville, J., Newman, M., Peacock, A., Cho, J. and Hatfield, K. (2011)

531   Evaluation and application of anion exchange resins to measure groundwater

532   uranium flux at a former uranium mill site. Water Research 45(16), 4866-4876.

533

534   Takahashi, H., Uchimiya, H. and Hihara, Y. (2008) Difference in metabolite levels

535   between photoautotrophic and photomixotrophic cultures of Synechocystis sp. PCC

536   6803 examined by capillary electrophoresis electrospray ionization mass

537   spectrometry. Journal of Experimental Botany 59(11), 3009-3018.

538   United States Environmental Protection Agency (USEPA) (2008) Test Methods for

539   Evaluating Solid Waste, Physical/Chemical Methods, Washington D.C.

540   United States Geological Survey (USGS) (2011) Mineral Commodity Summaries 2011,

541   Reston, VA.

542   van de Meene, A.M.L., Hohmann-Marriott, M.F., Vermaas, W.F.J. and Roberson, R.W.

543   (2006) The three-dimensional structure of the cyanobacterium Synechocystis sp

544   PCC 6803. Archives of Microbiology 184(5), 259-270.

545   Vermaas, W. (1996) Molecular Genetics of the Cyanobacterium Synechocystis sp. PCC

546   6803: Principles and Possible Biotechnology Applications. Journal of Applied

547   Phycology 8(4-5), 263-273.

548   Vermaas, W.F.J. (2001) Encyclopedia of Life Sciences, pp. 245-251, John Wiley & Sons,

549   Ltd, London.

550   Wijffels, R.H., Kruse, O. and Hellingwerf, K.J. (2013) Potential of Industrial

551   Biotechnology with Cyanobacteria and Eukaryotic Microalgae. Current Opinion in

552   Biotechnology 24(3), 405-413.

553   Wong, W.T., Chan, W.I., Liao, P.H., Lo, K.V. and Mavinic, D.C. (2006) Exploring the

554   Role of Hydrogen Peroxide in the Microwave Advanced Oxidation Process;

555   Solubilization of Ammonia and Phosphates. Journal of Environmental Engineering

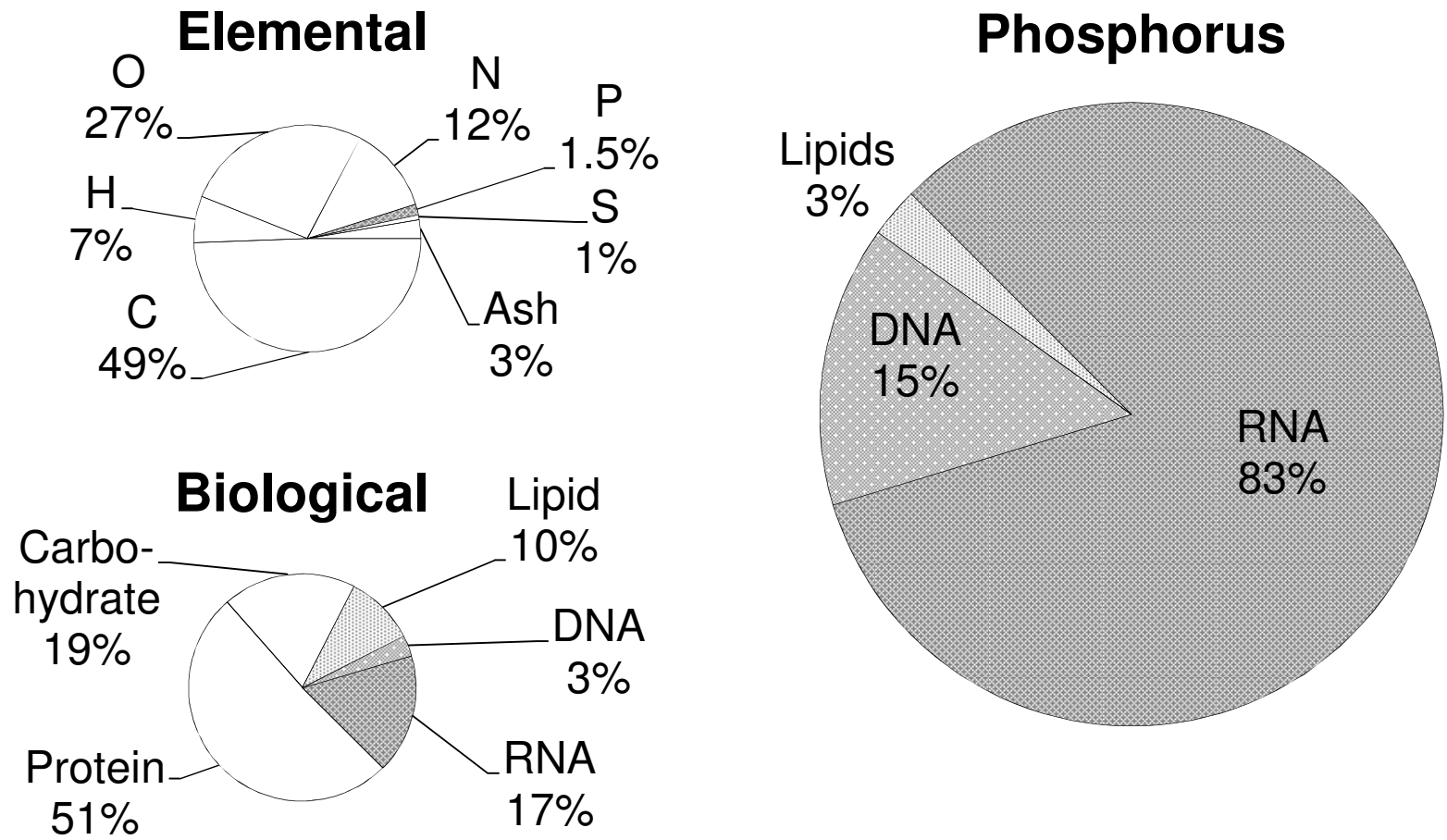556   and Science 5(6), 459-465.

557

Figure 1 – The estimated location of P within *Synechocystis* sp. PCC 6803 shown on the right determined by the elemental (Kim et al. 2010) and biological (Shastri and Morgan 2005) composition shown on the left. All numbers given are percent by weight of the total biomass (left) or total P in the biomass (right). A majority of cellular P is in RNA, and only small amounts are in lipids. Thus, almost all P is in the primary residuals after lipid extraction, not in the lipid extract.
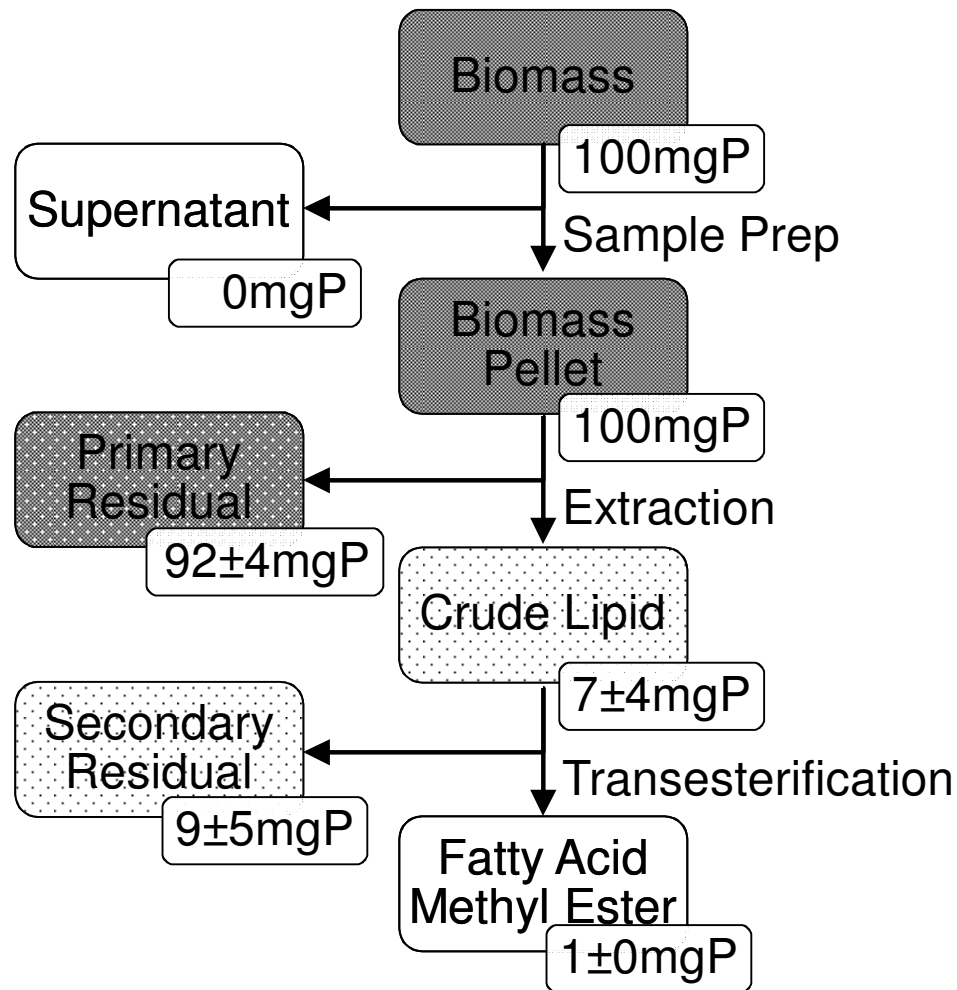
Figure 2 – The fate of 100 mg of starting P through the lipid extraction process. Most of the P remained with the biomass in the primary residual, although some was associated with the crude lipid remains in the secondary residual. The FAME only contained about 1% of the starting P.
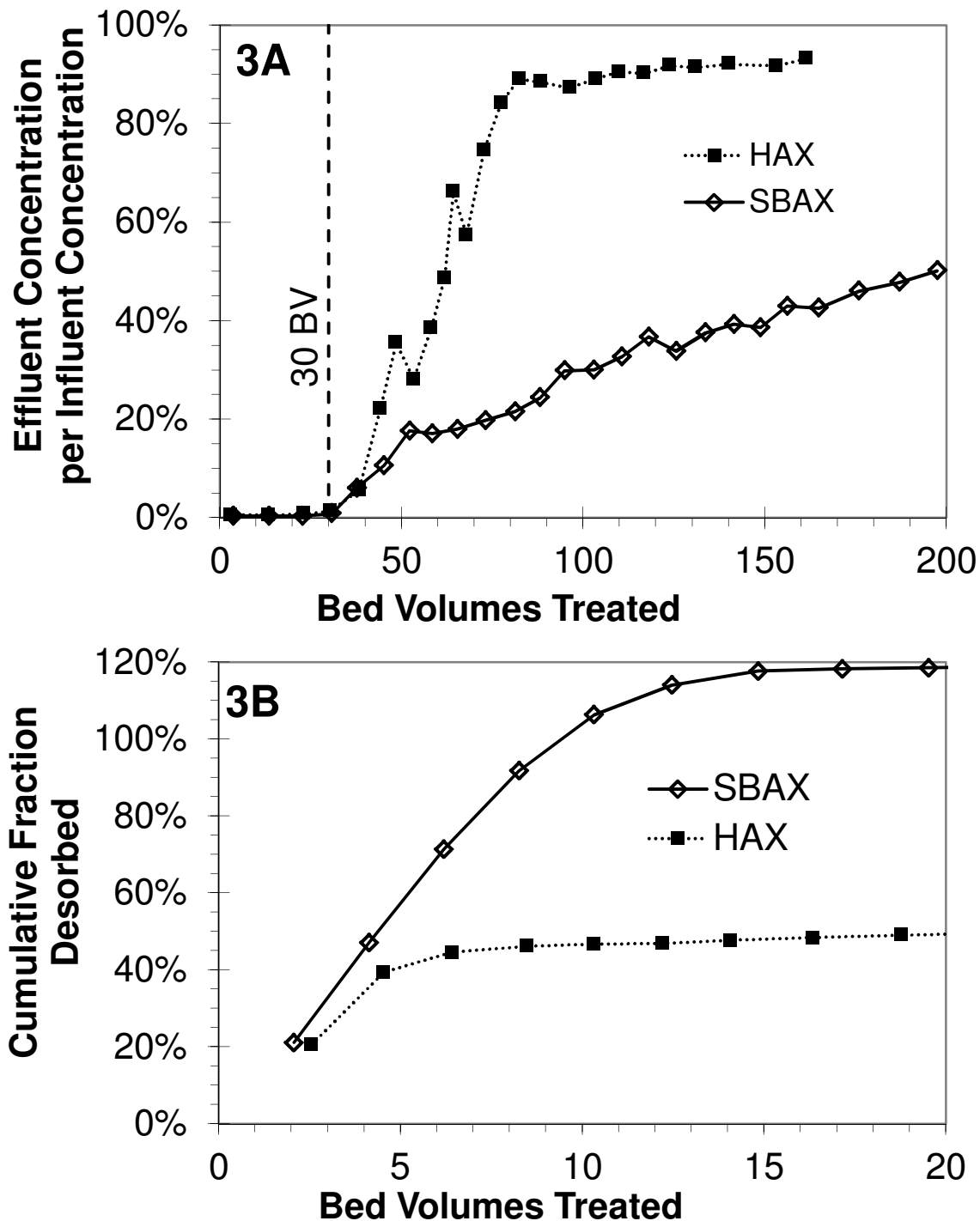
Figure 3 – Performance of an iron hydr(oxide) impregnated anion exchange (HAX) resin (squares) and a strong-base anion exchange (SBAX) resin (diamonds) for recovering phosphate from DI water. (A) Uptake of phosphate by fresh resin in column test. Uses hydraulic loading rate of 30 BV/hr, an initial P concentration of 80 mgP/L, and influent pH 5. (B) Desorption of phosphate from resin by 0.1 N KOH for HAX or 0.1 N NaCl for SBAX with hydraulic loading rate of 6 BV/hr, normalized to mass of P sorbed. The HAX resin shows higher affinity for P during sorption, but the SBAX releases more P upon elution.
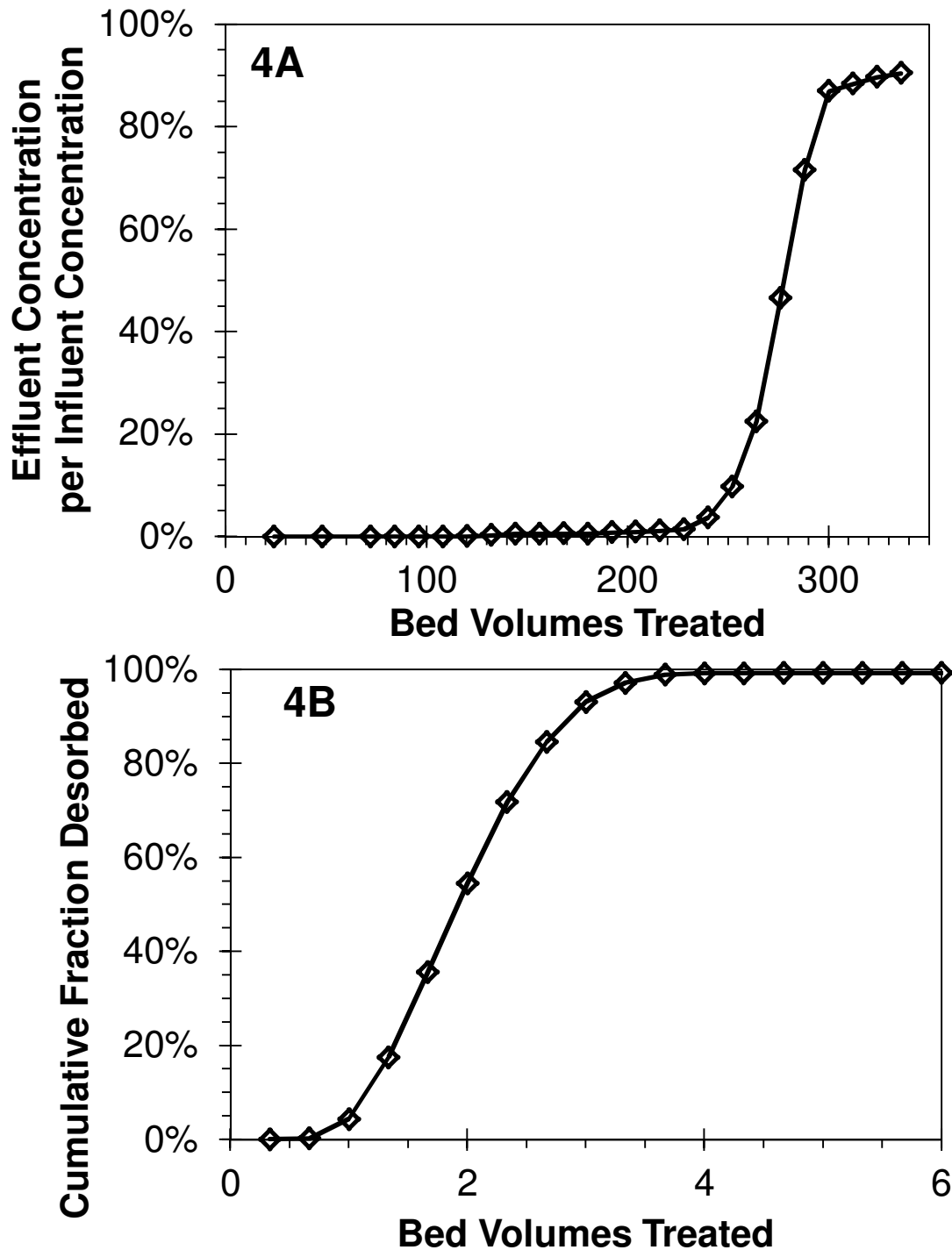
Figure 4 – Enhanced P recovery from DI water on SBAX resin by improving operating conditions. (A) Uptake of phosphate by fresh resin in column test. Uses hydraulic loading rate of 3 BV/hr, an initial P concentration of 100 mgP/L, and influent pH 8. (B) Desorption of phosphate from resin by 1 N NaCl at a hydraulic loading rate of 2 BV/hr, normalized to mass P sorbed. The steep breakthrough after a long bed run is optimal for P recovery, and subsequent elution in few bed volumes gives an 80-fold increase in P concentration.
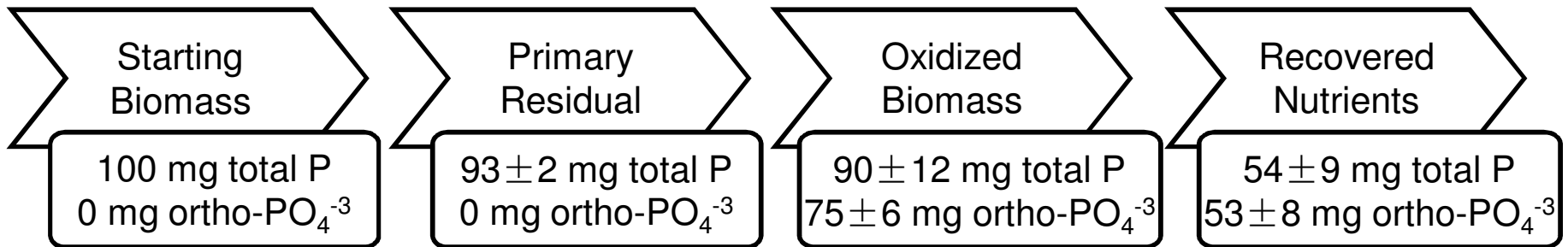
Starting Biomass	Primary Residual	Oxidized Biomass	Recovered Nutrients
100 mg total P 0 mg ortho-PO_4^{-3}	93 ± 2 mg total P 0 mg ortho-PO_4^{-3}	90 ± 12 mg total P 75 ± 6 mg ortho-PO_4^{-3}	54 ± 9 mg total P 53 ± 8 mg ortho-PO_4^{-3}

Figure 5 – Process step yields of total P and ortho-PO_4^{3-} for 100 mg starting P through the P-recovery process using advanced oxidation and SBAX. Nearly all cellular P was found in the primary residual after lipid extraction. Advanced oxidation transformed a majority of the P to recoverable and beneficial ortho-PO_4^{3-}. SBAX resin could then sorb and elute a concentrated nutrient solution. The overall tested P-recovery process could capture more than 50% of the starting P in a beneficial form.